Biophysical and Biochemical Approach to Locating an Inhibitor Binding Site on Cholesteryl Ester Transfer Protein

David Cunningham, Wen Lin, Lise R. Hoth, Dennis E. Danley, Roger B. Ruggeri, Kieran F. Geoghegan, Boris A. Chrunyk, and James G. Boyd*

Pfizer Global Research and Development, Groton, Connecticut 06340. Received April 22, 2008; Revised Manuscript Received June 20, 2008

Cholesteryl ester transfer protein (CETP) transfers neutral lipids between different types of plasma lipoprotein. Inhibitors of CETP elevate the fraction of plasma cholesterol associated with high-density lipoproteins and are being developed as new agents for the prevention and treatment of cardiovascular disease. The molecular basis of their function is not yet fully understood. To aid in the study of inhibitor interactions with CETP, a torcetrapib-related compound was coupled to different biotin-terminated spacer groups, and the binding of CETP to the streptavidin-bound conjugates was monitored on agarose beads and in a surface plasmon resonance biosensor. CETP binding was poor with a 2.0 nm spacer arm, but efficient with polyethyleneglycol spacers of 3.5 or 4.6 nm. The conjugate based on a 4.6 nm spacer was used for further biosensor experiments. Soluble inhibitor blocked the binding of CETP to the immobilized drug, as did preincubation with a disulfide-containing covalent inhibitor. To provide a first estimate of the binding site for torcetrapib-like inhibitors, CETP was modified with a disulfide-containing agent that modifies Cys-13 of CETP. Mass spectrometry of the modified protein indicated that a single half-molecule of the disulfide was covalently bound to CETP, and peptide mapping after digestion with pepsin confirmed previous reports based on mutagenesis that Cys-13 was the site of modification. Modified CETP was unable to bind to the biosensor-mounted torcetrapib analog, indicating that the binding site on CETP for torcetrapib is in the lipid-binding pocket near the N-terminus of the protein. The crystal structure of CETP shows that the sulfhydryl group of Cys-13 resides at the bottom of this pocket.

INTRODUCTION

Cardiovascular disease is the major cause of premature death in Western societies (*1*). Decades of epidemiological analysis has led to the recognition of multiple distinct risk factors for this syndrome, among which unhealthful elevation of the level of low-density lipoprotein (LDL) cholesterol is the best-known example. This can be treated successfully with statins, which block cholesterol production in the liver, but it still represents only about 30% of the total risk for acquiring the disease. There remains an urgent need for therapies that reduce other elements of the risk burden.

One example is suboptimal levels of high-density lipoprotein (HDL) cholesterol. HDL collect cholesterol from the vascular periphery, and return it (as cholesteryl esters) to the liver for excretion. Despite some advances, there are not yet any approved drugs that elevate the level of HDL cholesterol successfully enough (and in a manner sufficiently free of undesirable side effects) to make major inroads against atherosclerotic disease. Currently, however, there are intensive efforts to evaluate inhibitors of cholesteryl ester transfer protein (CETP) for this purpose.

CETP is a circulating hydrophobic glycoprotein with a polypeptide molecular mass of 53 kDa and three or four N-linked glycans. It transfers neutral lipids between lipoproteins of different classes (other functions await recognition), and reductions in this activity by drug action or genetic change lead to an elevation of HDL cholesterol. When a CETP inhibitor (torcetrapib) was coadministered with atorvastatin, quite dramatic changes in the plasma lipid profile were obtained of a kind corresponding to a highly desirable shift in the levels of both biomarkers (*2*). Torcetrapib, unfortunately, was recently withdrawn from development because of surprising adverse events (*3*), but it continues to be medically and scientifically important to elucidate the function of CETP at a molecular level and the manner in which its inhibitors bind to it and block its function.

Kinetic analysis of CETP function indicated that it is a shuttle protein (*4*), optionally binding to lipoproteins of different classes, extracting a small number of molecules of their predominant neutral lipids in exchange for lipids previously bound, and presumably existing as a soluble protein when not bound to a lipoprotein. A recent report of its crystal structure suggested how these functions might occur, showing that neutral lipids are carried in a 6 nm tunnel formed inside the protein's elongated body, while each orifice of the tunnel is plugged with an amphiphilic phospholipid (*5*). Keen interest now centers on how CETP inhibitors bind to the protein and affect its function as a lipid shuttle.

Several important clues are already available. Torcetrapib has been shown to increase the relative affinity of CETP for HDL by a factor of 5 (*6*). As a shuttle carrier must have finely balanced relative affinities for the different states that it populates, this effect is clearly sufficient to disable lipid transfer by CETP. It is also known that torcetrapib binds to CETP with 1:1 stoichiometry (*6*), but the binding pocket that it occupies on CETP has not been determined.

CETP possesses two large binding pockets for neutral lipids which form a continuous interior cavity within the protein (*5*), but are demarcated from each other by a constriction in the cavity that has been termed the neck. To date, there have been no direct reports of the structures of CETP-inhibitor complexes, but there has been biochemical and mutagenesis-based evidence that two distinct disulfide containing inhibitors each modify Cys-

* Corresponding author. Tel: 860-441-1580. Fax: 860-441-3858. E-mail: james_g_boyd@pfizer.com.

10.1021/bc800165n CCC: $40.75
Published on Web 07/23/2008

13 in the N-terminal region of CETP (*7, 8*). Another report suggested that a mercurial cholesterol analog inhibits by modifying Cys-333 in the C-terminal lipid binding region (*9*). In the present study, a close analog of torcetrapib was adapted for use in a biosensor instrument by coupling it to biotin-terminated spacers of different lengths, and the resulting conjugates were characterized for their ability to bind CETP. The ability to measure the binding of CETP to an immobilized inhibitor provided a basis for experiments probing the ability of different inhibitors to compete with one another for binding sites, and has led to the discovery that torcetrapib apparently occupies the same pocket as one of the covalent inhibitors for which the site of action was previously implied by mutagenesis and was directly determined in the present study.

EXPERIMENTAL SECTION

CETP Mutant 444. A mutant form of CETP (C1A, C131A, N88D, N240D, N341D) was prepared as described (*5*). The expressed protein, designated CETP 444, was composed of the 493-residue polypeptide given in Genbank accession M30185 with the five mutations as listed. Amino-acid numbering (including the mutations) refers to mature CETP lacking the 17-residue signal sequence, i.e., the eighteenth residue of the gene product is designated Cys-1. The mutant showed activity equal to that of recombinant wild-type CETP in cholesteryl ester transfer assays. For mass spectrometry of the intact protein, it was deglycosylated using peptide N-glycosidase F.

Reagents and Conditions. Guanidine hydrochloride (Sigma Ultra) and iodoacetamide were purchased from Sigma (St Louis, MO). Hydrochloric acid and Tris base were from J. T. Baker (Phillipsburg NJ). DTT was from BioVectra (PEI, Canada). TFA was from Applied Biosystems (Foster City, CA). All other solvents were from J. T. Baker or Applied Biosystems were used as purchased. Phosgene (2.0 M in toluene) was purchased from Fluka (St. Louis, MO), and 6-amino-1-hexanol and *tert*-butyl dicarbonate were from Aldrich. *N*-Fmoc-8-Amino-3,6-dioxaoctanoic acid was from Chem-Impex (Wood Dale, IL). 1-Amino-11-azido-3,6,9-trioxoundecane was from Toronto Research Chemicals (North York, Ontario, Canada). NHS-LC-Biotin and TFP-PEO-Biotin were purchased from Pierce (Rockford, IL). Boc-6-Amino-1-hexanol was prepared from commercially available *tert*-butyl dicarbonate and amino alcohol as described (*10*).

NMR was performed on a 400 MHz field strength spectrometer from Varian Inc. (Palo Alto, CA) in CD_3OD or $CDCl_3$. Chemical shifts are reported in parts-per-million (ppm). Residual solvent was used as reference (CD_3OD = 3.32 ppm, $CDCl_3$ = 7.27 ppm). Preparative HPLC was performed using a BISCHOFF (Atlanta, GA) C_{18} column (50 × 20 mm, part # B025 0F185PS050), eluting with a linear slope gradient of water/acetonitrile/TFA (95:5:0.1 to 20:80:0.1) over 10 min, then isocratic 80% acetonitrile for 5 min, and flow rate of 10 mL/min). Analytical samples for liquid chromatography electrospray mass spectrometry (LC ESMS) were dissolved in methanol. 5−10 μL each of these were injected onto a Phenomenex 4.6 × 50 mm C_{18} Jupiter column and eluted using a linear gradient from 0.1% TFA, 5% acetonitrile in water to 100% acetonitrile over 10 min with a flow rate of 1 mL/min. Mass detection was performed using a Micromass LCT spectrometer employing external calibration with sodium iodide/cesium iodide clusters to determine experimental masses. Observed peaks were evaluated by summing those scans at one-half peak height. Compound purity was assessed by C_{18} reversed phase HPLC (RP HPLC) methods using diode array UV detection. Biotinyl compounds were >89% pure when measured at 214 nm and >99% pure when measured at 250 nm.

Preparation of Affinity Columns. A stock solution of biotinyl ligand was prepared by dissolving compound **8**, **9**, or **13** (0.5 μmol) in 2.5 mL ethanol and diluting with 7.5 mL phosphate buffered saline (pH 7.0). An aliquot of the stock solution (5 μL) was diluted with 95 μL methanol and set aside as an HPLC standard. A 1 mL HiTrap Streptavidin HP column (GE Healthcare, catalog # 17−5112−01) was pre-equilibrated with 10 mL of 20% ethanol in pH 7.0 phosphate buffer. The 10 mL of ligand stock solution was passed over the column using a syringe at a flow rate of about 1 mL/min and the flow-through fraction collected. The column was washed with 10 mL of 20% ethanol in phosphate buffer and the eluant collected. The stock solution, flow-through, and wash fractions were assayed by RP HPLC. No ligand was detected in the eluants indicating complete loading on the column.

(±) Benzyl [(2*R*,4*S*)-2-ethyl-6-(trifluoromethyl)-1,2,3,4-tetrahydroquinolin-4-yl]carbamate (1). 4-Trifluoromethylaniline (1.2 g, 7.4 mmol) and propionaldehyde (0.5 g, 8.6 mmol) were combined in dichloromethane (30 mL) and treated with anhydrous sodium sulfate (2.5 g). After stirring 1 h at room temperature, the reaction mixture was filtered and to the resulting solution was added *N*-vinyl-*O*-benzylcarbamate (1 equivalent) and a drop of borontrifluoride etherate. After stirring for 90 min at room temperature the reaction mixture was concentrated onto silica gel employing a rotary evaporator and purified by silica gel chromatography eluting with 5−10% ethyl acetate in hexanes to afford 1.0 g of the racemic product (47%). ^{1}H NMR ($CDCl_3$): δ 7.32 − 7.41 (m, 5H), 7.22 (dd, 1H, *J* = 8.3, 2.1 Hz), 6.46 (d, 1H, *J* = 8.51 Hz), 5.18 (s, 2 H), 5.03 (td, 1H, *J* = 10.5, 5.5 Hz), 4.87 (d, 1H, *J* = 9.6 Hz), 4.06 (bs, 1H), 3.35 − 3.45 (m, 1H), 2.32 (ddd, 1H, *J* = 12.3, 5.5, 2.6 Hz), 1.54 (d, 1H, *J* = 6.4 Hz), 1.51 − 1.58 (m, 1 H), 1.45 (td, 1H, *J* = 11.6 Hz), 0.98 (t, 3H, *J* = 7.5 Hz).

Benzyl [(2*R*,4*S*)-2-ethyl-1-(trifluoroacetyl)-6-(trifluoromethyl)-1,2,3,4-tetrahydroquinolin-4-yl]carbamate (2). Compound **1** (1.0 g, 2.6 mmol) and triethylamine (1 mL, 7.2 mmol) were dissolved in 30 mL of dichloromethane and cooled in an ice/water bath as trifluoroacetic anhydride (0.5 mL, 3.5 mmol) was added. After 4 h, the reaction mixture was combined with an aqueous 1 N HCl solution, and the organic phase washed with a saturated aqueous $NaHCO_3$ solution, dried over $MgSO_4$, filtered and concentrated under reduced pressure to afford the racemic product (85%). The enantiomers were separated by regular phase HPLC using a Chiralcel OD column eluting with 20% isopropanol in heptane. The later eluting peak contains the desired THQ enantiomer with the (2*R*, 4*S*) stereochemistry. ^{1}H NMR ($CDCl_3$): δ 7.60 (s, 1 H), 7.57 (d, 1 H, *J* = 7.5 Hz), 7.39 (m, 6 H), 5.19 (s, 2 H), 4.97 (d, 1 H, *J* = 9.1 Hz), 4.79 (bs, 1 H), 4.66 (bs, 1 H), 2.69 (m, 1 H), 1.48 (m, 1 H), 1.37 (m, 2 H), 0.97 (t, 3 H, *J* = 7.5 Hz).

(2*R*,4*S*)-2-Ethyl-1-(trifluoroacetyl)-6-(trifluoromethyl)-1,2,3,4-tetrahydroquinolin-4-amine (3). Compound **2** (1.0 g, 2.1 mmol) was dissolved in 30 mL each of absolute ethanol and cyclohexene. The resulting solution was treated with 10% Pd on carbon (200 mg, 50% by weight with water) and heated at reflux. After 1 h, the reaction mixture was filtered through a pad of Celite and concentrated under reduced pressure to afford the title compound. ^{1}H NMR ($CDCl_3$): δ 7.82 (s, 1H), 7.58 (ddd, 1H *J* = 8.3, 1.4, 0.7 Hz), 7.33 (bs, 1H), 4.71 (bs, 1H), 3.83 (dd, 1H, *J* = 11.4, 5.2 Hz), 2.64 (ddd, 1H, *J* = 12.5, 8.8, 5.3 Hz), 1.42 − 1.51 (m, 1H), 1.29 − 1.41 (m, 1H), 1.18 (bs, 1H), 0.88 (t, 3H, *J* = 7.5 Hz).

***N*-[3,5-Bis(trifluoromethyl)benzyl]-*N*-[(2*R*,4*S*)-2-ethyl-1-(trifluoroacetyl)-6-(trifluoromethyl)-1,2,3,4-tetrahydroquinolin-4-yl]acetamide (4).** Compound **3** (0.5 g, 1.5 mmol) and 3,5-(bis)trifluoromethylbenzaldehyde (0.36 g, 1.5 mmol) were combined in 40 mL of 1,2-dichloroethane at room temperature. After 1 h, sodium triacetoxyborohydride (0.21 g, 7.5 mmol) was added and the mixture stirred for 18 h. An aqueous 2 N

KOH solution was added to the reaction mixture, the organic phase was separated, dried over $MgSO_4$, filtered and concentrated under reduced pressure to afford 0.65 g crude amine. The amine was dissolved in 1.0 mL pyridine and 20 mL dichloromethane, and the resulting mixture cooled with an ice/water bath. Acetyl chloride (0.5 mL, 7.0 mmol) was added slowly by syringe and the reaction stirred at room temperature for 4 h. Aqueous 1 N HCl solution was added to the reaction mixture, the organic layer was separated, washed once with an aqueous saturated sodium bicarbonate solution, dried over magnesium sulfate, filtered and concentrated under reduced pressure. The resulting material was purified by chromatography on silica eluting with 20% ethyl acetate in hexanes to afford the title compound (44%). ^{1}H NMR ($CDCl_3$): [~2:1 mixture of rotamers] δ 7.74 − 7.88 (m, 1H), 7.67 (s, 1H), 7.65 − 7.73 (m, 1H), 7.48 (bs, 1H), 7.27 (s, 1H), 5.59 (d, 1H, J = 16 Hz), 4.84 (dd, 1H, J = 11.9, 4.7 Hz), 4.55 − 4.71 (m, 1H), 3.96 (d, 1H, J = 16.2 Hz), 2.35 (bs, H), 2.26 (bs, 1H), 2.24 (s, 2H), 2.08 (s, 1H), 1.43 − 1.61 (m, 1H), 1.27 − 1.43 (m, 2H), 0.78 (t, 3H, J = 7.4 Hz).

***N*-[3,5-Bis(trifluoromethyl)benzyl]-*N*-[(2*R*,4*S*)-2-ethyl-6-(trifluoromethyl)-1,2,3,4-tetrahydroquinolin-4-yl]acetamide (5).** Compound **4** (400 mg, 0.66 mmol) was dissolved in 10 mL THF, combined with 5 mL of an aqueous 2 N LiOH solution, and stirred at room temperature for 4 h. The reaction mixture was concentrated under reduced pressure, the residue diluted with water and $MgSO_4$, filtered, and concentrated under reduced pressure to afford the title compound. ^{1}H NMR ($CDCl_3$): [~2:1 mixture of rotamers] δ 7.54 − 7.83 (m, 3H), 7.21 − 7.27 (m, 1H), 6.92 − 7.01 (m, 1H), 6.49 − 6.57 (m, 1H), 5.26 (dd, 1H, J = 11.8, 5.6 Hz), 4.59 − 4.89 (m, 1H), 3.99 − 4.14 (m, 1H), 3.99 − 4.29 (m, 1H), 3.40 (bs, 1H), 2.38 (s, 2H), 2.14 (s, 1H), 1.94 − 2.09 (m, 1H), 1.37 − 1.66 (m, 3H), 0.93 (t, 2H, J = 7.4 Hz), 0.89 (t, 1H, J = 7.7 Hz).

(6-[(*tert*-Butoxycarbonyl)amino]hexyl) (2*R*,4*S*)-4-{acetyl[3,5-bis(trifluoromethyl)benzyl]amino}-2-ethyl-6-(trifluoromethyl)-3,4-dihydroquinoline-1(2H)-carboxylate (6a). To a solution of 300 mg compound **5** in 5 mL toluene was added 3 mL of 20% phosgene (6 mmol) in toluene. The reaction was refluxed for 6 h, cooled to room temperature, and the excess phosgene was driven into a trap by a stream of nitrogen. The residual solvent was evaporated on rotovap followed by high vacuum, leaving the carbamoyl chloride as a waxy solid. LCMS showed it to be a mixture of 95% carbamoyl chloride and 5% **5,** which is stable at room temperature for at least 30 days (ESMS: calculated m/z for $[M+H]^+$ = 575.11, found = 575.22). To 50 mg carbamoyl chloride (0.087 mmol) was added 1.0 mL toluene, 95 mg Boc-6-amino-1-hexanol (0.44 mmol) and 0.1 mL DIEA. The reaction was refluxed for 24 h, cooled, evaporated, dissolved in 0.5 mL methanol and directly purified by preparative HPLC as described in Reagents and Conditions. Collected fractions were analyzed by analytical LCMS and those judged as having adequate purity were pooled and lyophilized. The purity of the product was 90% as determined by HPLC at 215 nm. Yield = 15 mg (23%). ^{1}HNMR (CD_3OD): δ 7.92 (s, 2H), 7.84 (s, 1H), 7.6 (dd, 2H), 7.06 (s, 1H), 5.3 (d, 1H, J = 16 Hz), 5.14 (dd, 1H), 4.35 (m, 1H), 4.29 (d, 1H, J = 16 Hz), 4.16 (t, 2H), 2.99 (t, 2H), 2.28 (m, 1H), 2.26 (s, 3H), 1.67 (m, 4H), 1.5−1.3 (m, 8H), 1.40 (s, 9H), 0.72 (t, 3H). ESMS: calculated m/z for $[M+H]^+$ = 756.30, found = 756.51.

6-Aminohexyl (2*R*,4*S*)-4-{acetyl[3,5-bis(trifluoromethyl)benzyl]amino}-2-ethyl-6-(trifluoromethyl)-3,4-dihydroquinoline-1(2*H*)-carboxylate (6b), TFA Salt. Boc protected urethane **6a** (15 mg) was treated with 0.5 mL TFA for 10 min at room temperature. The TFA was evaporated under a stream of nitrogen, then at high vacuum. The purity of the amine TFA salt was 90% as determined by HPLC at 214 nm. Yield = 15 mg (100%). ESMS: calculated m/z for $[M+H]^+$ = 656.25, found = 656.38. HRMS: calculated m/z for $[M+H]^+$ = 656.2529, found = 656.2526.

(6-({[2-(2-Aminoethoxy)ethoxy]acetyl}amino)hexyl) (2*R*,4*S*)-4-{acetyl[3,5-bis(trifluoromethyl)benzyl]amino}-2-ethyl-6-(trifluoromethyl)-3,4-dihydroquinoline-1(2*H*)-carboxylate (7), TFA Salt. To a solution of 7.0 mg (18 μmol) Fmoc-8-amino-3,6-dioxaoctanoic acid in 36 μL of a 0.5 M DMF solution of HOBT/HBTU (18 μmol) was added 10 μL (60 μmol) DIEA. After 2 min, 6.0 mg (9.1 μmol) of TFA salt **6b** was added and the solution allowed to react for 1 h. The reaction solution was diluted with 10 mL ethyl ether, and washed with 0.1 M HCl, 0.1 M $NaHCO_3$, saturated NaCl, and dried over $MgSO_4$. The ether was filtered and concentrated to an oily solid. The solid was treated with 0.1 mL 30% piperidine/DMF for 20 min, then 30 μL acetic acid was added to quench the reaction. The solution was fractionated by direct injection onto a C_{18} preparative HPLC column as for **5**, and appropriate fractions were pooled and lyophilized. Yield = 2.0 mg (28%). ESMS: calculated m/z for $[M+H]^+$ = 801.33, found = 801.36.

(6-{[6-({5-[(3a*S*,4*S*,6a*R*)-2-Oxohexahydro-1*H*-thieno[3,4-*d*]imidazol-4-yl]pentanoyl}amino)hexanoyl]amino}hexyl)(2*R*,4*S*)-4-{acetyl[3,5-bis(trifluoromethyl)benzyl]amino}-2-ethyl-6-(trifluoromethyl)-3,4-dihydroquinoline-1(2*H*)-carboxylate (8). To a solution of 5.0 mg (7.6 μmol) TFA salt **6b** in 50 μL DMF was added 10 mg (22 μmol) NHS-LC-Biotin and 5 μL DIEA. After 1 h, the product was purified by direct injection onto a C_{18} preparative HPLC column as for **5**. Appropriate fractions were pooled and lyophilized. HPLC purity at 214 nm = 94%, at 250 nm >99%. Yield = 6.2 mg (65%). ESMS: calculated m/z for $[M+H]^+$ = 995.41, found = 995.61. HRMS: calculated m/z for $[M+H]^+$ = 995.4145, found = 995.4142.

(8,11,27-Trioxo-31-[(3a*S*,4*S*,6a*R*)-2-oxohexahydro-1*H*-thieno[3,4-*d*]imidazol-4-yl]-16,19,22-trioxa-7,12,26-triazahentriacont-1-yl) (2*R*,4*S*)-4-{acetyl[3,5-bis(trifluoromethyl)benzyl]amino}-2-ethyl-6-(trifluoromethyl)-3,4-dihydroquinoline-1(2*H*)-carboxylate (9). To a solution of 4.0 mg (6.1 μmol) TFA salt **6b** in 50 μL DMF was added 16 mg (23 μmol) TFP-PEO-Biotin (Pierce, catalog # 21336) and 5 μL DIEA. After 1 h, the product was purified by direct injection onto a C_{18} preparative HPLC column as for **5**. Appropriate fractions were pooled and lyophilized. HPLC purity at 214 nm = 89%, at 250 nm >99%. Yield = 4.0 mg (55%). ESMS: calculated m/z for $[M+H]^+$ = 1184.51, found = 1184.75. HRMS: calculated m/z for $[M+2H]^{+2}$ = 592.7609, found = 592.7632.

(8,17,20,36-Tetraoxo-40-[(3a*S*,4*S*,6a*R*)-2-oxohexahydro-1*H*-thieno[3,4-*d*]imidazol-4-yl]-10,13,25,28,31-pentaoxa-7,16,21,35-tetraazatetracont-1-yl) (2*R*,4*S*)-4-{acetyl[3,5-bis(trifluoromethyl)benzyl]amino}-2-ethyl-6-(trifluoromethyl)-3,4-dihydroquinoline-1(2*H*)-carboxylate (10). TFP-PEO-Biotin was allowed to react with 2.0 mg (2.2 μmol) of TFA salt **7** as described for the synthesis of **9**. HPLC purity at 214 nm = 94%, at 250 nm >99%. Yield = 1.5 mg (51%). ESMS: calculated m/z for $[M+H]^+$ = 1329.73, found = 1329.59. HRMS: calculated m/z for $[M+2H]^{+2}$ = 665.2979, found = 665.3000.

Methyl [(2*S*,4*R*)-1-(13-azido-5,8,11-trioxa-2-azatridecan-1-oyl)-2-ethyl-6-(trifluoromethyl)-1,2,3,4-tetrahydroquinolin-4-yl]carbamate (12). In a 1.5 mL Eppendorf tube 150 mg (0.50 mmol) of methyl [(2*S*,4*R*)-2-ethyl-6-(trifluoromethyl)-1,2,3,4-tetrahydroquinolin-4-yl]carbamate (**11**) (*11*) was dissolved in 0.10 mL THF. *p*-Nitrochloroformate (200 mg, 2.0 equiv) was added and the resulting solution was shaken at 40 °C for 16 h. The THF was evaporated and residue was dissolved in 1.5 mL methanol, 0.35 mL DIEA. 400 mg (4.0 equiv) 1-amino-11-azido-3,6,9-trioxoundecane was added and the resulting solution was shaken at 70 °C for 48 h. The product was purified by

direct injection onto preparative HPLC as for compound **5** except a shallower solvent gradient to 50% acetonitrile was employed. Yield = 99 mg (36%). ESMS: calculated *m/z* for $[M+H]^+$ = 547.25, found = 547.24.

Methyl [(2*S*,4*R*)-1-{15,22-dioxo-26-[(3a*S*,4*S*,6a*R*)-2-oxohexahydro-1H-thieno[3,4-d]imidazol-4-yl]-5,8,11-trioxa-2,14,21-triazahexacosan-1-oyl}-2-ethyl-6-(trifluoromethyl)-1,2,3,4-tetrahydroquinolin-4-yl]carbamate (13). 4.2 mg (7.7 μmol) of compound **12** was dissolved in 2 mL THF. Three mg Pd/C was added and the mixture shaken under 50 psi H_2 for 5 h. The reaction was filtered through a plug of celite and evaporated. LCMS showed >99% conversion of the azide to the amine (ESMS: calculated *m/z* for $[M+H]^+$ = 521.26, found = 521.22). The amine was dissolved in 100 μL DMF and 10 μL DIEA. NHS-LC-Biotin (14 mg, 4.0 equiv) was added and the solution shaken for 1 h at room temperature The product was purified by direct injection onto preparative HPLC as for compound **5**. HPLC purity at 214 nm = 95%, at 250 nm >99%. ESMS: calculated *m/z* for $[M+H]^+$ = 860.42, found = 860.57. HRMS: calculated *m/z* for $[M+H]^+$ = 860.4198, found = 860.4196.

Covalent Modification of CETP. CETP (18 μM) was incubated with **14** (50 μM) in 20 mM Tris, 150 mM NaCl, pH 7.5 for 36 h at room temperature, after which it was dialyzed exhaustively against the same buffer at 4 °C.

Biosensor Analyses. SPR measurements were performed using a Biacore 3000 system (GE Healthcare, Piscataway, NJ). In typical experiments, biotinylated drug analogs were immobilized onto standard Biacore streptavidin-coated biosensor chips. CETP binding was measured at 25 °C in 20 mM Tris pH 7.4, 150 mM NaCl, 0.005% Tween 20, 1% DMSO using a flow rate of 100 μL/min. The underivatized streptavidin surface was used as a reference. Surfaces were regenerated between injections by two sequential three-second pulses of 0.1% SDS. Data were processed using Scrubber 2 software (BioLogic Software) to y-zero, x-align and double reference against buffer injections and a streptavidin surface lacking any immobilized ligand. Kinetic analyses were conducted using BIAeval software (GE Healthcare, Piscataway, NJ.).

Acetone Precipitation of CETP. HCl (0.005 mL, 0.5 M) was added to 0.042 mL of CETP (2.4 mg/mL) to give a final HCl concentration of 0.05 M. 0.150 mL of cold acetone was added and the sample was allowed to stand at −20 °C for 2 h, after which the sample was centrifuged for 10 min at 14,000 rpm in a microfuge. The supernatant was discarded and the pellet was dried in a centrifugal concentrator to remove residual acetone.

Peptic Digestion/Reduction. The acetone precipitate (~0.1 mg CETP) was dissolved in 0.1 mL of 0.05 M HCl, 8 M guanidine hydrochloride, and incubated at 50 °C for 15 min. The sample was diluted to 3 M guanidine hydrochloride, 0.001 mL of pepsin at 2 mg/mL was added, and the sample was digested for 19 h at 23 °C. The samples was then divided into two portions: (i) Nonreduced, non-neutralized sample: 0.002 mL water was added to 0.010 mL of the pepsin digest. (ii) Reduced sample: 0.001 mL 1 M Tris base and 0.001 mL 1 M DTT was added to 0.01 mL of the pepsin digest.

Reversed-Phase Liquid Chromatography−Mass Spectrometry. Peptide mapping by reversed-phase HPLC-MS was conducted by capillary HPLC using a Vydac type 218MS5.510 column (0.5 × 100 mm) running at 0.005 mL/min on an Agilent 1100 chromatograph based on a Model G1376A capillary pump and interfaced with a Thermo Finnigan LCQ ion-trap mass spectrometer. The HPLC solvents were: A, 0.02% TFA; B, 0.02% TFA in acetonitrile. From initial conditions of 1.6% B (0−2 min), the gradient consisted of steps from 1.6−35% B (2−100 min), and 35−80% B (100−110 min). The standard Finnigan electrospray interface was modified by replacing the sample needle with a coated fused silica tip (TaperTip; part number TT150−50−50-CE-5, New Objective Inc., Woburn, Massachusetts). The LCQ was controlled by Xcalibur 1.2 software (Thermo Finnigan) and set to perform data-dependent MS/MS analysis ("triple play") as described. Peptides were identified by searching the Swiss-Prot sequence database using Sequest as implemented under license by Thermo Finnigan (Sequest Browser), or the Mascot search engine (Matrix Sciences) (*12*).

Size-Exclusion Chromatography−Mass Spectrometry. SEC-MS was conducted with a Phenomenex Bio-SEC-S3000 column (300 × 4.6 mm) run at 0.2 mL/min on an Agilent 1100 chromatograph based on a Model G1312A binary pump and interfaced with a Micromass LCT electrospray/time-of-flight mass spectrometer. The HPLC solvent was 0.045% TFA in 40% acetonitrile. The LCT was controlled by MassLynx 4.0 software (Waters).

RESULTS

Affinity Ligand Synthesis. Compound **4**, a close-in analog of torcetrapib (Scheme 1), was selected as the starting structure for elaboration to potential affinity ligands. Internal (unpublished) torcetrapib SAR had shown that the methoxycarbonyl at the tetrahydroquinoline (THQ) 4-amino position could be replaced with acetyl without loss of affinity for CETP. More importantly for the present investigations, replacement of the ethyl chain of the THQ 1 position carbamate with longer alkyl chains only slightly reduced CETP binding. Hence, we investigated the value of placing different biotin-terminated spacer arms in this substituent. Condensation of 4-trifluoromethylaniline with propionaldehyde followed by addition to *N*-vinyl-*O*-benzylcarbamate provided a direct route to racemic cis-4-aminocarbobenzyloxy (Cbz) protected THQ **1**. Trifluoroacetylation of the THQ 1-amine affords an intermediate that can be readily separated into its constitutive enantiomers by chiral HPLC methods. Thus **2** was obtained, which following hydrogenation provides the suitably protected primary amine **3**. Reductive coupling of **3** with 3,5-bis-trifluoromethylbenzaldehyde followed by acetylation of the alkylated 4-amino group led to intermediate **4**. Removal of the trifluoroacetyl group with lithium hydroxide delivered key THQ **5**. Reaction of **5** with phosgene in toluene followed by evaporation of the solvent provided a carbamoyl chloride crude product in about 95% purity. We found that the THQ carbamoyl chloride reacted readily with amines, but the product ureas had significantly reduced affinity for CETP. Synthesis of high affinity urethane compounds was significantly more difficult, but reaction with excess *N*-Boc protected 6-aminohexanol in refluxing toluene did provide compound **6a** in modest yield. Finally, removal of the Boc group of compound **6a** with TFA afforded amine salt **6b**.

Putative CETP affinity ligands were prepared as shown in Scheme 2. TFA salt **6b** was coupled directly with a long chain *N*-hydroxysuccinimidyl ester of biotin (NHS-LC-Biotin) to produce compound **8**, which was purified by reverse phase HPLC. Similarly, **6b** was coupled to Fmoc-8-amino-3,6-dioxaoctanoic acid with HBTU activation, and the resulting intermediate was deblocked with piperidine/DMF and purified by preparative HPLC to provide amine salt **7**. Amines **6b** and **7** were allowed to react with the tetrafluorophenyl (TFP) ester of a PEG-biotin reagent (TFP-PEO-Biotin) to prepare compounds **9** and **10**, respectively. Control urea compound **13** was prepared from chiral THQ **11** (*11*), which features the opposite THQ stereochemistry of torcetrapib (Scheme 3). Activation of the THQ nitrogen of **11** with *p*-nitrophenylchloroformate followed by reaction with a commercially available heterobifunctional linker provided urea azide **12**, a compound that lacks

Scheme 1[a]

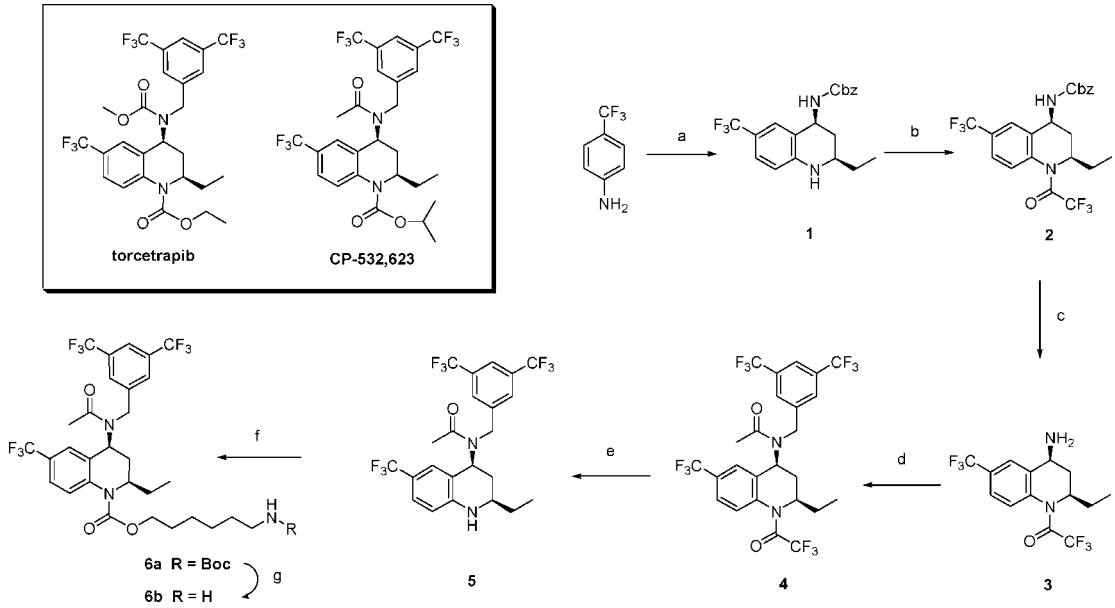

[a] Reagents and conditions: (a) (i) propionaldehyde (1.2 equiv), anhyd. Na_2SO_4, DCM, room temp, 1 h, (ii) *N*-vinyl-*O*-benzylcarbamate (1 equiv), cat. BF_3 Et_2O, room temp, 1.5 h, 47%; (b) (i) TFAA (1.3 equiv), DCM, 0−5 °C, 4 h, 85%, (ii) chiral column resolution; (c) wet 10% Pd/C, cyclohexane/EtOH, reflux, 1 h; (d) (i) 3,5-(bis)trifluoromethylbenzaldehyde (1.0 equiv), $NaBH(AcO)_3$, DCE, room temp, 18 h, (ii) AcCl (5.0 equiv), pyridine/DCM, 0 °C then room temp, 4 h, 44%; (e) LiOH, THF/water, room temp, 4 h; (f) (i) $COCl_2$ (10 equiv), toluene, reflux, 6 h, (ii) Boc-6-amino-1-hexanol (5 equiv), toluene, DIEA, reflux 24 h, 23%; (g) neat TFA, 5 min, 100%.

Scheme 2[a]

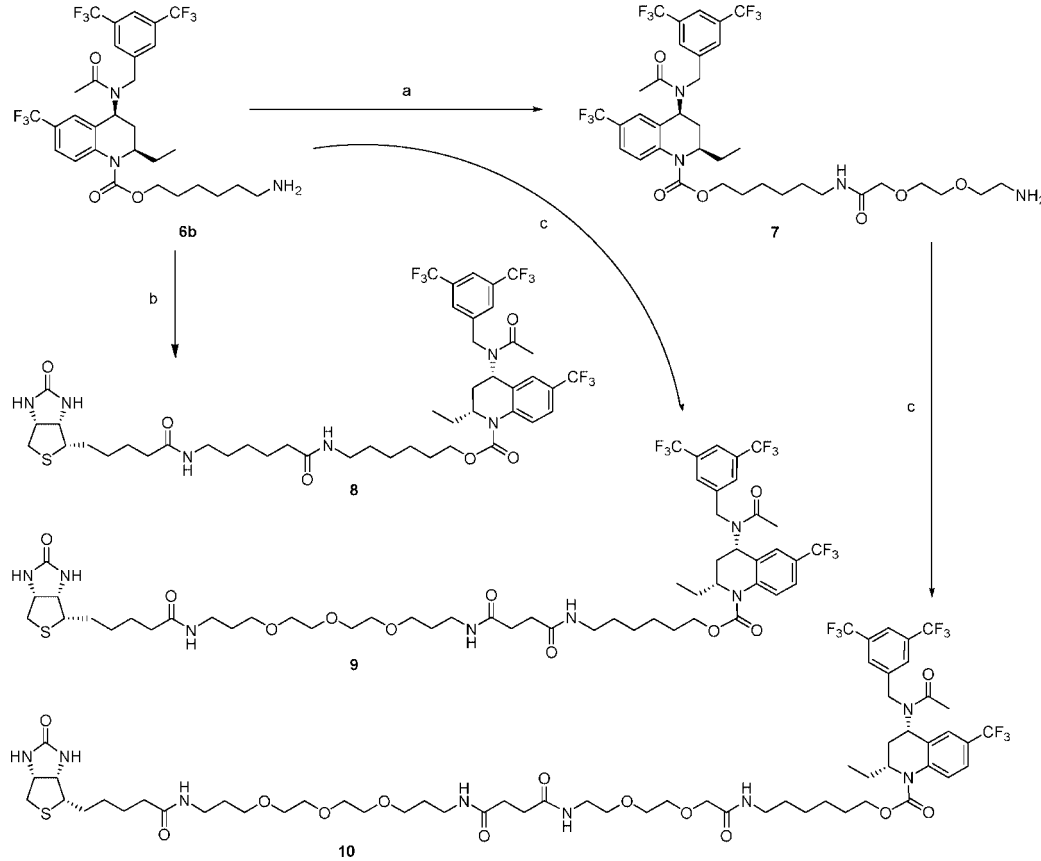

[a] Reagents and conditions: (a) (i) Fmoc-8-amino-3,6-dioxaoctanoic acid, HBTU (2 equiv.), DIEA, DMF, room temp, 1 h, (ii) piperidine (20 equiv), 28%; (b) NHS-LC-Biotin (3 equiv), DIEA, DMF, room temp, 1 h, 65%; (c) TFP-PEO-Biotin (3.8 equiv.), DIEA, DMF, room temp, 1 h, 51−55%.

detectable CETP affinity for CETP. Catalytic hydrogenation of the azide to primary amine followed by acylation with NHS-LC-Biotin provided the desired negative control compound **13**.

CETP Inhibition and Affinity Column. Compounds **6a**, **8**, **9**, and **10**, were tested for their ability to inhibit the CETP-mediated transfer of ^{3}H-labeled cholesteryl oleate from HDL

Scheme 3[a]

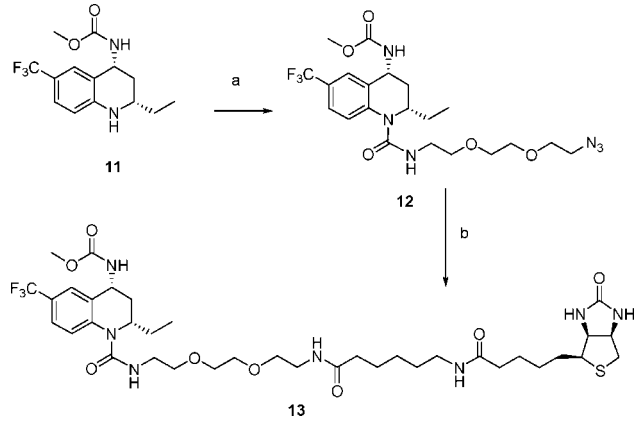

[a] Reagents and conditions: (a) (i) *p*-nitrophenyl chloroformate (2.0 equiv), THF, 40 °C, 15 h, (ii) 1-amino-11-azido-3,6,9-trioxoundacane (4.0 equiv), MeOH, DIEA, 70 °C, 48 h, 36%; (b) (i) H_2, cat. Pd/C, THF, room temp, 5 h, (ii) NHS-LC-biotin (3.5 equiv), DMF, DIEA, room temp, 1 h.

Table 1. Effects of Immobilization and Spacer Arm Length on CETP Binding

compound	phase	IC50[b] (μM)	% CETP bound[c]	capacity (μg/mL)	spacer length[e] atoms[d]	spacer length[e] nm
6a	solution	1.5	NA[a]	NA	NA	NA
8	agarose	2.3	20	75	16	2.1
9	agarose	2.6	>98	1100	28	3.5
10	solution	0.72	NA	NA	37	4.6
12	solution	>300	NA	NA	NA	NA
13	agarose	ND	19	70	21	2.5
none	agarose	NA	<3	<10	NA	NA

[a] NA = not applicable; ND = not determined. [b] Average of two determinations. [c] Reported as the percent missing from the flow-through fraction and washings as measured by SDS−PAGE, and absorbance at 280 nm following a 0.375 mg load. Additional 0.375 mg aliquots of CETP were used to determine column capacity. [d] Number of atoms between the THQ 1 position and the carboxyl group of the biotin affinity handle. [e] Estimated for fully extended conformation using average bond length = 1.48 Å and the formula (average bond length)(cos 35)(# atoms + 1).

to LDL or VLDL in 90% human plasma (*13*). All three compounds showed similar affinities for CETP, with IC_{50} values in the low micromolar range (Table 1). By comparison, the reported IC_{50} value for torcetrapib is 47 nM (*6*), indicating that the aminohexanol-derived spacers caused a 30- to 50-fold loss in binding affinity. Control compound **12,** which had the opposite stereochemistry of torcetrapib and lacked the 3,5-(bis)trifluoromethylbenzyl group, did not inhibit CETP.

Biotinyl compounds **8**, **9**, and **13** were evaluated as potential ligands for immobilization of CETP. A 0.5 mg sample of each compound was allowed to bind to 1 mL of Streptavidin Sepharose, a maximum loading density of 0.5 mg/mL agarose (~0.5 mM). Solutions of purified CETP were passed over the columns as well as over a column of Streptavidin Sepharose containing no biotinyl ligand, and the flow-through fractions were assayed for protein using SDS-PAGE and absorbance at 280 nm. When 0.37 mg of CETP was passed over Streptavidin Sepharose lacking affinity ligand, >97% of the protein was recovered from the flow-through and wash fractions, indicating no detectable binding to the matrix (Table 1). When 0.37 mg of CETP was passed over the column prepared with ligand **8**, 0.30 mg (81%) was recovered in the flow-through. Additional aliquots of protein were passed over the column of immobilized **8**, but no additional CETP bound, indicating that its total capacity for CETP was 0.07 mg/mL. This result was essentially identical to that seen with a column made from biotinylated

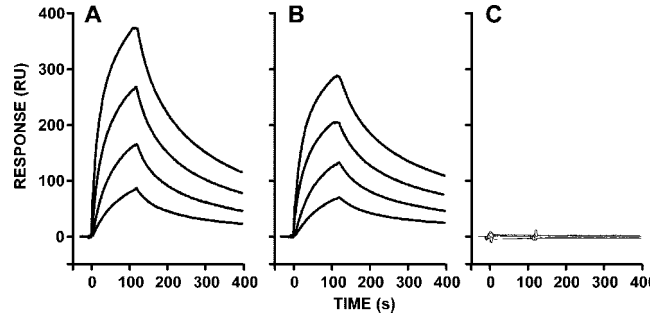

Figure 1. The effect of spacer arm length on the binding of CETP to immobilized inhibitor. Wild-type CETP at 1.7, 0.56, 0.18, and 0.06 μM was injected over (A) compound **10** (spacer 4.6 nm); (B) compound **9** (spacer 3.5 nm), and (C) compound **8** (spacer 2.9 nm). Each compound was immobilized to give a surface density of ~150 RU on the streptavidin biosensor surfaces.

control compound **13**, and suggests that CETP binding to columns of immobilized **8** and **13** was compound-dependent but nonspecific, and likely due to hydrophobic interaction with the THQ rather than to specific binding of the immobilized torcetrapib analog. In contrast, when CETP was passed over columns of immobilized **9**, essentially all of the protein bound to the column and none was detected in the flow-through fraction. By passing additional aliquots of protein over a column of **9** until overloading occurred, the CETP capacity was determined to be about 1.1 mg/mL. When dissolved in plasma, ligands **8** and **9** had similar potencies in the CE transfer assay, but **8** did not specifically bind CETP when immobilized. This strongly suggested that there was a dependence on linker length, and that the 16-atom spacer of **8** was too short for the THQ group to access the torcetrapib binding pocket when the biotin residue was bound to streptavidin.

Biosensor Analysis. Initial SPR experiments evaluated the effect of spacer length on CETP binding. When CETP was injected over biotinyl compounds **8**, **9**, and **10** immobilized on a streptavidin-coated biosensor, binding results were similar to those seen when the compounds were immobilized on Streptavidin Sepharose. No specific CETP binding was observed with **8** (Figure 1), confirming that its 16-atom spacer is too short to allow the THQ group to reach the torcetrapib binding pocket. While both **9** and **10** bound CETP (Figure 1), compound **10** had approximately 25% greater binding capacity than **9**, suggesting that the 37-atom spacer of **10** allowed greater access to the torcetrapib site than did the 28-atom spacer of **9**. All subsequent SPR experiments used immobilized **10**. A kinetic analysis of CETP binding at concentrations ranging from 2.8 μM to 0.1 μM indicated that binding was somewhat complex. However, a reasonable global fit could be made using the 1:1 Langmuir model that indicated a K_D of approximately 0.3 μM with an on-constant of 22 000 ± 200 $M^{-1}s^{-1}$ and an off-constant of 0.0064 ± 0.0001 s^{-1} (data not shown). This value correlated well with the IC_{50} of 0.7 μM obtained for **10** in the transfer assay (Table 1). Though IC_{50} is dependent on the conditions of the assay, which are different from those used in the SPR assay, a value consistent in magnitude to the calculated K_D suggests that the assay is relevant to specific binding of the compound and target. For a competitive inhibitor K_D relates to IC_{50} by the equation $K_D = IC_{50}/(1+[S]/K_m)$. When CETP was preincubated with an equimolar concentration of either torcetrapib (not shown) or its close analog CP-532,623 (*14*), binding to **10** was substantially inhibited (Figure 2), providing good evidence that immobilized **10** binds specifically to CETP in the same pocket as torcetrapib.

The test of ability to bind to immobilized **10** could then be used to survey inhibitors for evidence of binding in the

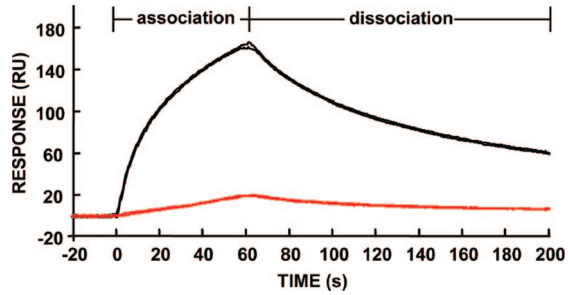

Figure 2. Preincubation with inhibitor prevents CETP binding to immobilized torcetrapib analog. Mutant CETP 444 at 1 μM was preincubated 30 min with (red) or without (black) torcetrapib analog CP-532,623 (1 μM) and injected in duplicate over immobilized 10.

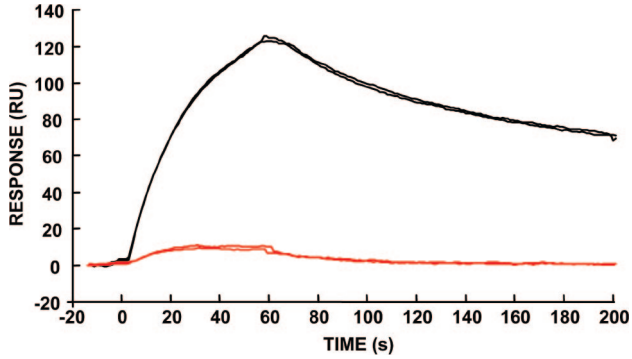

Figure 3. Modification with **14** prevents CETP binding to immobilized torcetrapib analog. Mutant CETP 444 modified with compound **14** (red) or unmodified control (black) each at 1 μM was injected in duplicate over immobilized compound **10**.

Scheme 4

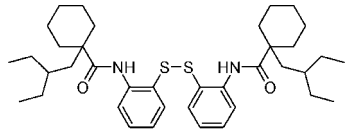

14

torcetrapib pocket. When the reportedly covalent disulfide inhibitor **14** (compound 4 of reference (*7*)) was preincubated with CETP, it blocked binding of CETP to immobilized **10** (Figure 3) and lowered its cholesteryl ester transfer activity by >90% (data not shown). The action of this compound was investigated in more detail to enhance its value as an indicator of the binding site of torcetrapib.

Stoichiometry of Modification. Site-directed mutagenesis implicated Cys-13 as the reaction site on CETP for **14** (*7*) (see Scheme 4 for structure), but could not exclude the possibility of additional modifications at other cysteine residues. To check the stoichiometry of modification, modified CETP 444 was subjected to electrospray/time-of-flight mass spectrometry using size-exclusion chromatography in 40% acetonitrile as the desalting method (Figure 4). To obtain interpretable spectra, it was necessary to remove the lone glycan on Asn-296 of CETP 444 using peptide N-glycosidase F. For unmodified CETP 444, the mass of 53 052 Da (Figure 4A) agreed acceptably well with the theoretical value of 53 046 Da, which assumes a disulfide bond between Cys-143 and Cys-184 and conversion of Asn-296 to Asp-296 during deglycosylation. The minor peak came from protein lacking residues 1−3, as verified by Edman sequencing (mass obsd. 52 765 Da; mass theor. 52 760 Da)

Peaks in the mass spectrum of CETP 444 treated with **14** gained 326 Da (major) and 321 Da (minor), respectively,

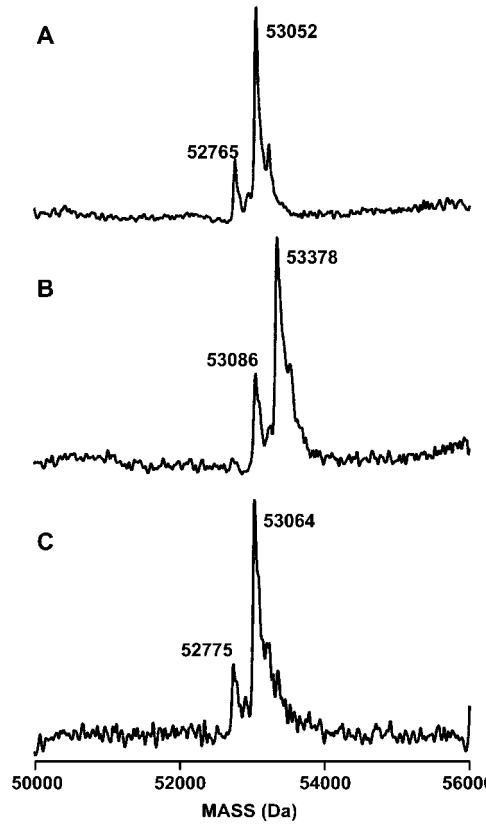

Figure 4. Mass spectrometry of CETP 444 (A) before and (B) after modification with **14** and (C) after treatment of the modified protein with dithiothreitol. The theoretical mass for deglycosylated unmodified CETP 444 (major peak) was 53046 Da, and for the same protein lacking amino acids 1−3, it was 52760 Da. The theoretical mass increase resulting from the formation of a mixed disulfide with a half-molecule of **14** was 317 Da.

consistent in this method with addition of a single half-molecule of **14** as a mixed disulfide with a protein thiol (theoretical increase 317 Da) (Figure 4B). Treatment with dithiothreitol reversed the modification, supporting the interpretation (Figure 4C).

Site of Modification by 14. The site at which **14** modified CETP 444 was determined by peptide mapping, using pepsin as the agent of digestion. Pepsin was chosen not only for its broad specificity and preference for hydrophobic sites, but also because digesting CETP at pH 2 lowered the risk of disulfide interchange reactions. In the map of the modified protein (Figure 5), new peaks in the 100−108 min range (see asterisks in Figure 5B) were attributed on the bases of novelty, mass and MS/MS-derived sequencing (not shown) to fragments containing Cys-13 disulfide-linked to the half-molecule of **14**. The peaks at 100, 104 and 108 min were attributed to fragments 1−20, 4−20 and 11−20 of CETP 444, respectively, each modified by the addition of 317.5 Da at Cys-13. Also detected, but in much lower abundance, were the modified peptides 1−21, 4−21 and 11−21. No other cysteine was modified. Peptides from unmodified CETP 444 containing Cys-13 as a free thiol were absent from the digest of the modified form (not shown). Treating the digest of the modified protein with dithiothreitol abolished the modification, confirming that it was based on a disulfide (Figure 5C).

DISCUSSION

SPR-based biosensors detect changes in refractive index that occur when molecules in solution bind to their immobilized partners in the molecular layer adjacent to the biosensor surface

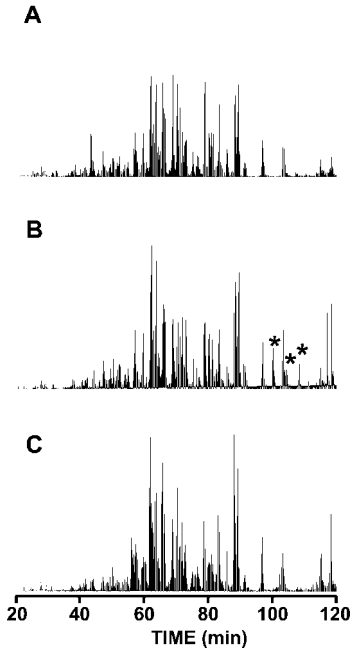

Figure 5. Base peak chromatograms from LC-MS peptide mapping analysis of (A) CETP 444; (B) CETP 444 after modification with **14**; and (C) after treatment of the modified CETP with dithiothreitol. Asterisks in panel B mark the three major peaks attributed to peptides containing the mixed disulfide bond between Cys-13 of CETP and one-half-molecule of **14**. From left to right, the three marked peaks were attributed to peptides 1−20, 4−20, and 11−20 of CETP 444 (see Table 2 for data related to the identifications).

(*15*). Early SPR technology was limited to detecting the capture of macromolecules, but refinements now make it possible to detect directly the binding of small molecules to immobilized proteins in many systems. Largely because of the availability of this technology, kinetic analyses of interactions between candidate drugs and their targets are an increasingly important aspect of drug discovery (*16*). Biosensors can now provide these analyses for a wide variety of targets beyond the classical cases of slow-binding enzyme inhibitors (*17*) and membrane-bound receptors. However, in some cases development of a method for direct biosensor kinetics is hindered by difficulties in obtaining stable and active immobilized protein or by problems associated with compound aggregation or compound binding to fluidics and reference surfaces. CETP and its inhibitors presented all of these of difficulties. (D. Cunningham, unpublished).

When direct kinetic biosensor methods are not possible, indirect inhibitor affinity data can sometimes be obtained from solution affinity experiments in which protein and ligand are mixed at various ligand concentrations and the mixtures are allowed to come to equilibrium. When the mixtures are injected over an immobilized ligand, the initial rate of protein binding to the immobilized ligand is proportional to the free (unliganded) protein concentration. For optimum results, the free protein must bind the immobilized compound to give a sufficiently robust signal when present in concentrations at or below the K_d for the competing inhibitor.

While immobilized small molecule approaches can circumvent the problems listed above, their use in SPR techniques has been limited due to the need to synthesize tagged ligands that retain useful receptor affinity when bound to SPR chips (for examples see *18–25*). In general, ligand development is an empirical process but it is aided greatly by the availability of direct structural information or compound series SAR. In the present examples we drew upon in-house (unpublished) SAR in the torcetrapib series which suggested that CETP could accommodate long linear spacer groups at the torcetrapib THQ 1 position. Thus compound **6a** was synthesized and found to exhibit an IC_{50} of 1.5 μM in a cholesteryl ester transfer assay (Table 1). The measured IC_{50} for torcetrapib in this assay is near 50 nM (*13*) indicating that **6a** suffers a 30-fold reduction in binding affinity for CETP, perhaps due to some unfavorable interactions with the protein. Nonetheless, low micromolar affinity was judged sufficient for further ligand development.

Hydrophilic spacers of different lengths were placed between biotin and the drug-like component to generate affinity ligands **8**, **9**, and **10**. In solution these ligands showed similar affinities for CETP as measured by the transfer assay but the length of the spacer arm proved to be critical for efficient CETP binding when immobilized. When the conjugates were bound to streptavidin, either on agarose matrices or biosensor surfaces, it was found that a 2.1 nm (extended length) polyethyleneglycol-based spacer was not long enough to reach the torcetrapib pocket in CETP (Figure 1). While both the 3.5 nm spacer of compound **9** and the 4.6 nm spacer of compound **10** were sufficient to allow binding to a biosensor surface, the 4.6 nm linker apparently allowed better access and provided the greatest CETP binding capacity. Preincubation of CETP with free torcetrapib analog prevented binding to immobilized **10** on a biosensor surface (Figure 2), suggesting that binding was specific and based on occupancy of the site that accommodates torcetrapib. Although the binding of CETP to the immobilized compound appeared to be complex (data not shown), a reasonable fit could be obtained using a simple 1:1 binding analysis. CETP bound to immobilized **10** with an affinity that was very similar to its affinity for **10** in solution (K_d = 0.3 μM, as compared to a transfer assay IC_{50} of 0.7 μM). This binding proved to be more than adequate for use in an affinity resin, where high immobilization densities and relatively low flow rates contribute to extensive rebinding, However, when **10** was immobilized in a biosensor for the solution affinity measurements for which it was designed, the signal was not robust at the low CETP concentrations required. This may have been in part due to variable losses of the hydrophobic CETP to instrument fluidics when injected at low concentrations.

The linker lengths reported in Table 1 are for fully extended *anti* conformations of all sp^3 hybridized linker atoms, but it is *gauche* conformations that predominate for polymers of ethylene

Table 2. Peptides Detected with the +317.2 Da Modification at Cys-13 by Peptic Peptide Mapping of CETP 444 Modified with a Half-Molecule of Disulfide 14.

fragment	sequence[a]	mass theor. (Da)[b]	mass obsd. (Da)	ions detected/theoretical[c]
1−21	ASKGTSHEAGIVC*RITKPALL	2468.4	2468.4	15/40
1−20	ASKGTSHEAGIVC*RITKPAL	2355.3	2355.5	12/36
4−21	GTSHEAGIVC*RITKPALL	2182.2	2182.0	2/30
4−20	GTSHEAGIVC*RITKPAL	2069.1	2069.1	8/28
11−21	IVC*RITKPALL	1542.9	1543.0	4/18
11−20	IVC*RITKPAL	1429.9	1430.0	10/16

[a] Asterisk indicates that the modification was at Cys-13. [b] Masses are monoisotopic. [c] Singly charged b- and y-type sequence ions in MS/MS of the peptide.

oxide (*26*). Dynamics simulation experiments performed on PEG-based linkers have shown that extended linker lengths are often overestimated and that the effective linker length of PEG linkers is probably 60−80% of that calculated here (*27*). Even taking this adjustment into account, the magnitude of the linker length dependence observed for compounds **8**, **9**, and **10** is still striking. One can rationalize this result by referring to the recently published crystal structure of CETP (*5*). The structure reveals a 6.0 nm long tunnel which traverses the length of the protein and binds two molecules of cholesteryl ester and two molecules of phospholipid. The tunnel can be accessed by either of two openings which allow entry and egress of lipid cargo molecules. The linker length data reported here support a model where torcetrapib affinity analogs enter through an opening and bind deep in the tunnel. When immobilized on an avidin support, the linker of **8** is not long enough to allow the tethered drug to reach the torcetrapib binding site (Figure 1 and Table 1). The lower CETP binding capacity observed for compound **9** relative to **10** may indicate that 3.5 nm linker length of **9** is near the minimum needed to access the torcetrapib binding site.

Despite this, the tethered torcetrapib analog proved quite valuable in another SPR application for surveying inhibitors of various chemotypes for evidence of binding either in the torcetrapib pocket or in distinct pockets (D. Cunningham, unpublished work). These experiments revealed that **14** blocks wild-type CETP binding to immobilized **10.** As **14** was thought to be a covalent inhibitor (*7*), it then became a convenient tool for the focus of the present study to locate primary sequence in proximity to the torcetrapib binding site. While a previous report provided indirect evidence for the involvement of Cys-13 in disulfide formation with a thioester closely related to **14**, the results presented demonstrated that **14** inactivates CETP by reacting with Cys-13. Mass spectrometry of the intact modified molecule demonstrated that **14** modified the simplified mutant CETP 444 with one-half-molecule of disulfide only, and peptide mapping after digestion with pepsin confirmed that the modified residue was Cys-13. Mutant CETP 444 so modified was inhibited for binding to immobilized torcetrapib analog, suggesting that torcetrapib also binds in the vicinity of Cys-13. The crystal structure of CETP (*5*) shows that indeed Cys-13 resides in the bottom of the N-terminal pocket that forms one end of the lipid-binding tunnel. This study shows that immobilized inhibitors can be useful probes in SPR even when the immobilized inhibitor has a relatively weak affinity for the target protein.

ACKNOWLEDGMENT

We are grateful to George Perkins for expert HRMS analyses.

LITERATURE CITED

(1) De Backer, G., Ambrosioni, E., Borch-Johnsen, K., Brotons, C., Cifkova, R., Dallongeville, J., Ebrahim, S., Faergeman, O., Graham, I., Mancia, G., Manger Cats, V., Orth-Gomer, K., Perk, J., Pyorala, K. L, Rodicio, J., Sans, S., Sansoy, V., Sechtem, U., Silber, S., Thomsen, T., and Wood, D. (2004) European guidelines on cardiovascular disease prevention in clinical practice. *Atherosclerosis 173*, 379–389.

(2) Brousseau, M. E., Schaefer, E. J., Wolfe, M. L., Bloedon, L. T., Digenio, A. G., Clark, R. W., Mancuso, J. P., and Rader, D. J. (2004) Effects of an inhibitor of cholesteryl ester transfer protein on HDL cholesterol. *N. Engl. J. Med. 350*, 1505–1515.

(3) Tall, A. R., Yvan-Charvet, L., and Wang, N. (2007) The failure of torcetrapib: Was it the molecule or the mechanism? *Arterioscler., Thromb., Vasc. Biol. 27*, 257–260.

(4) Connolly, D. T., McIntyre, J., Heuvelman, D., Remsen, E. E., McKinnie, R. E., Vu, L., Melton, M., Monsell, R., Krul, E. S., and Glenn, K. (1996) Physical and kinetic characterization of recombinant human cholesteryl ester transfer protein. *Biochem. J. 320*, 39–47.

(5) Qiu, X., Mistry, A., Ammirati, M. J., Chrunyk, B. A., Clark, R. W., Cong, Y., Culp, J. S., Danley, D. E., Freeman, T. B., Geoghegan, K. F., Griffor, M. C., Hawrylik, S. J., Hayward, C. M., Hensley, P., Hoth, L. R., Karam, G. A., Lira, M. E., Lloyd, D. B., McGrath, K. M., Stutzman-Engwall, K. J., Subashi, A. K., Subashi, T. A., Thompson, J. F., Wang, I.-K., Zhao, H., and Seddon, A. P. (2007) Crystal structure of cholesteryl ester transfer protein reveals a long tunnel and four bound lipid molecules. *Nat. Struct. Mol. Biol. 14*, 106–113.

(6) Clark, R. W., Ruggeri, R. B., Cunningham, D., and Bamberger, M. J. (2006) Description of the torcetrapib series of cholesteryl ester transfer protein inhibitors, including mechanism of action. *J. Lipid Res. 47*, 537–552.

(7) Okamoto, H., Yonemori, F., Wakitani, K., Minowa, T., Maeda, K., and Shinkai, H. (2000) A cholesteryl ester transfer protein inhibitor attenuates atherosclerosis in rabbits. *Nature 406*, 203–207.

(8) Hope, H. R., Heuvelman, D., Duffin, K., Smith, C., Zablocki, J., Schilling, R., Hegde, S., Lee, L., Witherbee, B., Baganoff, M., Bruce, C., Tall, A. R., Krul, E., Glenn, K., and Connolly, D. T. (2000) Inhibition of cholesteryl ester transfer protein by substituted dithiobisnicotinic acid dimethyl ester: Involvement of a critical cysteine. *J. Lipid Res. 41*, 1604–1614.

(9) Epps, D. E., and Vosters, A. F. (2002) The essential role of a free sulfhydryl group in blocking the cholesteryl site of cholesteryl ester transfer protein (CETP). *Chem. Phys. Lipids 114*, 113–122.

(10) Mattingly, P. G. (1990) Mono-protected diamines. Nα-tert-Butoxycarbonyl α,ω-alkanediamine hydrochlorides from amino alcohols. *Synthesis* 366–368.

(11) Damon, D. B., Dugger, R. W., Hubbs, S. E., Scott, J. M., and Scott, R. W. (2006) Asymmetric synthesis of the cholesteryl ester transfer protein inhibitor torcetrapib. *Org. Process Res. Dev. 10*, 472–480.

(12) Perkins, D. N., Pappin, D. J. C., Creasy, D. M., and Cottrell, J. S. (1999) Probability-based protein identification by searching sequence databases using mass spectrometry data. *Electrophoresis 20*, 3551–3567.

(13) Clark, R. W., Sutfin, T. A., Ruggeri, R. B., Willauer, A. T., Sugarman, E. D., Magnus-Aryitey, G., Cosgrove, P. G., Sand, T. M., Wester, R. T., Williams, J. A., Perlman, M. E., and Bamberger, M. J. (2004) Raising high-density lipoprotein in humans through inhibition of cholesteryl ester transfer protein: An initial multidose study of torcetrapib. *Arterioscler., Thromb., Vasc. Biol. 24*, 490–497.

(14) Kelley, R. M., McCarthy, K. E., Miller, S. A., Nesler, M. J., Schildknegt, K., Wager, C. B., and Zandi, K. S. (2004) The Synthesis of Isotopically Labeled CETP Inhibitors. *Synthesis and Applications of Isotopically Labelled Compounds*, Proceedings of the 8th International Symposium, Boston, MA, June 15, 2003, pp11−14. .

(15) Rich, R. L., and Myszka, D. G. (2007) Higher-throughput, label-free, real-time molecular interaction analysis. *Anal. Biochem. 361*, 1–6.

(16) Huber, W., and Mueller, F. (2006) Biomolecular interaction analysis in drug discovery using surface plasmon resonance technology. *Curr. Pharm. Des. 12*, 3999–4021.

(17) Morrison, J. F., and Walsh, C. T. (1988) The behavior and significance of slow-binding enzyme inhibitors. *Adv. Enzymol. Relat. Areas Mol. Biol. 61*, 201–301.

(18) Cannon, M. J., Myszka, D. G., Bagnato, J. D., Alpers, D. H., West, F. G., and Grissom, C. B. (2002) Equilibrium and kinetic analyses of the interactions between vitamin B12 binding proteins and cobalamins by surface plasmon resonance. *Anal. Biochem. 305*, 1–9.

(19) Gobi, K. V., and Miura, N. (2004) Highly sensitive and interference-free simultaneous detection of two polycyclic aromatic hydrocarbons at parts-per-trillion levels using a surface

plasmon resonance immunosensor. *Sens. Actuators, B 103*, 265–271.

(20) Jenssen, K., Sewald, K., and Sewald, N. (2004) Synthesis of marimastat and a marimastat conjugate for affinity chromatography and surface plasmon resonance studies. *Bioconjugate Chem. 15*, 594–600.

(21) Kaiser, T., Gudat, P., Stock, W., Pappert, G., Grol, M., Neumeier, D., and Luppa, P. B. (2000) Biotinylated steroid derivatives as ligands for biospecific interaction analysis with monoclonal antibodies using immunosensor devices. *Anal. Biochem. 282*, 173–185.

(22) Kanoh, N., Kyo, M., Inamori, K., Ando, A., Asami, A., Nakao, A., and Osada, H. (2006) SPR imaging of photo-cross-linked small-molecule arrays on gold. *Anal. Chem. 78*, 2226–2230.

(23) Miyashita, M., Shimada, T., Miyagawa, H., and Akamatsu, M. (2005) Surface plasmon resonance-based immunoassay for 17β-estradiol and its application to the measurement of estrogen receptor-binding activity. *Anal. Bioanal. Chem. 381*, 667–673.

(24) Schlecht, U., Nomura, Y., Bachmann, T., and Karube, I. (2002) Reversible surface thiol immobilization of carboxyl group containing haptens to a BIAcore biosensor chip enabling repeated usage of a single sensor surface. *Bioconjugate Chem. 13*, 188–193.

(25) Svedhem, S., Enander, K., Karlsson, M., Sjoebom, H., Liedberg, B., Loefas, S., Martensson, L.-G., Sjoestrand, S. E., Svensson, S., Carlsson, U., and Lundstroem, I. (2001) Subtle differences in dissociation rates of interactions between destabilized human carbonic anhydrase ii mutants and immobilized benzenesulfonamide inhibitors probed by a surface plasmon resonance biosensor. *Anal. Biochem. 296*, 188–196.

(26) Begum, R., Masatoki, S., and Matsuura, H. (1996) Conformational behavior of short poly(oxyethylene) compounds in formamide: a Raman spectroscopic study. *J. Mol. Struct. 384*, 115–120.

(27) Green, N. S., Reisler, E., and Houk, K. N. (2001) Quantitative evaluation of the lengths of homobifunctional protein cross-linking reagents used as molecular rulers. *Protein Sci. 10*, 1293–1304.

BC800165N